

Collective treatment of High Energy Thresholds in SUSY - GUTs .

A. Katsikatsou

*University of Athens, Physics Department, Nuclear and Particle Physics Section,
GR-15771 Athens, Greece*

Abstract

Supersymmetric GUTs are the most natural extension of the Standard model unifying electroweak and strong forces. Despite their indubitable virtues, among these the gauge coupling unification and the quantization of the electric charge, one of their shortcomings is the large number of parameters used to describe the high energy thresholds (HET), which are hard to handle. We present a new method according to which the effects of the HET, in any GUT model, can be described by fewer parameters that are randomly produced from the original set of the parameters of the model. In this way, regions favoured by the experimental data are easier to locate, avoiding a detailed and time consuming exploration of the parameter space, which is multidimensional even in the most economic unifying schemes. To check the efficiency of this method, we directly apply it to a SUSY SO(10) GUT model in which the doublet-triplet splitting is realized through the Dimopoulos-Wilczek mechanism. We show that the demand of gauge coupling unification, in conjunction with precision data, locates regions of the parameter space in which values of the strong coupling α_{strong} are within the experimental limits, along with a suppressed nucleon decay, mediated by a higgsino driven dimension five operators, yielding lifetimes that are comfortably above the current experimental bounds. These regions open up for values of the SUSY breaking parameters $m_0, M_{1/2} < 1 \text{ TeV}$ being therefore accessible to LHC.

1 Introduction

Grand unified theories (GUTs) provide a simple and elegant framework for the unification of strong, weak and electromagnetic forces. In addition, they offer a simple explanation of the electric charge and hypercharge assignments to the quarks and leptons in the Standard Model and combine its seekingly unrelated left and right - handed multiplets (five per family) into common representations of the larger unifying group. Moreover, their minimal supersymmetric versions, SUSY GUTs, lead to a successful gauge coupling unification at scales $M_{GUT} \approx 10^{16}$ GeV, which is impossible to realize without supersymmetry. Also, in the framework of particulate SUSY-GUTs, the lightness of the neutrinos can be explained and a mechanism for Baryogenesis through thermal Leptogenesis is offered as an alternative to Baryogenesis through electroweak phase transition, which requires large CP - violating phases.

In this note, our goal is to check the viability of SUSY GUTs, using electroweak precision and proton decay data by developing an integrated and simple scheme for the treatment of high energy thresholds (HET), which can be applicable, in principle, to any GUT model. In this scheme, the HETs are collectively parametrized by a small number of properly chosen variables, which are therefore easier to handle in phenomenological analyses. These are produced from the numerous parameters defining the HETs in a random way.

We employ our method to a SUSY - $SO(10)$ [1], which seems to be a very promising candidate for a unified description. Models based on $SO(10)$ unify all quarks and leptons of one family into one irreducible spinor representation, they give upper bounds on proton lifetime that still survive the current experimental bounds, they naturally incorporate the see-saw mechanism, reproducing the current neutrino oscillation data and explaining the lightness of the left-handed neutrinos with the sterile neutrino mass being of order M_{GUT} [2], and finally predict Yukawa unification [3], $\lambda_t = \lambda_b = \lambda_\tau = \lambda_{\bar{\nu}_\tau}$, for large $\tan\beta$. Our analysis is based on a minimal supersymmetric $SO(10)$ model first proposed in [4], whose low energy effective theory is the constrained MSSM.

As we have already noted, a common characteristic of all $SO(10)$ models is the inclusion of all quarks and lepton of one generation, along with the right handed neutrino, in the same spinorial, $\mathbf{16}$, representation. The $SO(10)$ generators belong to the adjoint representation $\mathbf{45}_V$.

As far as the content of the Higgs sector is concerned, there are two approaches that have been considered in the literature. Their difference rely on the way the Higgs mechanism is realized at the GUT scale. The first approach uses pairs of spinor Higgs multiplets in $\mathbf{16}_H + \overline{\mathbf{16}}_H$ representations to reduce the rank of the group [4–6], whereas

the other adopts a pair of $\mathbf{126}_H + \overline{\mathbf{126}}_H$ instead [7]. In both cases, a Higgs field in the $\mathbf{45}$ or the $\mathbf{54}$ representation is also needed, in addition, to further break $SO(10)$ to the Standard Model. Moreover, in order to build a viable model in $SO(10)$, one should always take into account that the Higgs multiplets of $SO(10)$ should include the two MSSM Higgs doublets H_u, H_d , which give masses to the up and down quarks respectively and additional Higgs fields, which are necessary to obtain the appropriate symmetry breaking pattern at the unification scale. The Higgs content of the particular model, which we will study, follows the first approach and is characterized as minimal. It consists of one Higgs multiplet A in the adjoint $\mathbf{45}_H$ representation, two pairs of $\mathbf{16}_H + \overline{\mathbf{16}}_H$ multiplets, named $C + \overline{C}, C' + \overline{C}'$, and two Higgs T_1, T_2 in the vector $\mathbf{10}_H$ representation.

$SO(10)$ is spontaneously broken to the Standard Model without intermediate breaking scales, as shown in Figure 1.

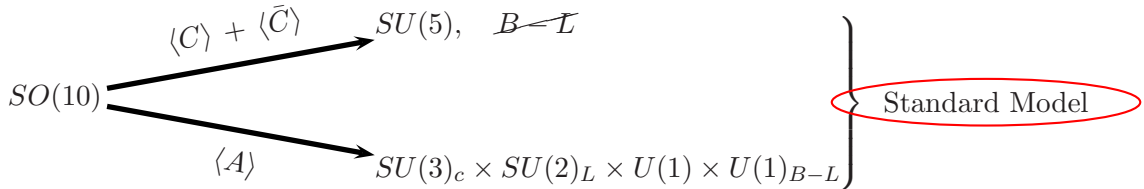


Figure 1: The breaking scheme of $SO(10)$ to Standard Model.

In general, there are at least four sectors that are needed in the Higgs superpotential to accomplish the $SO(10)$ breaking [4, 6]: the doublet-triplet-splitting sector $W_{2/3}$, the adjoint sector W_A , the spinor sector W_C and the adjoint-spinor coupling sector $W_{ACC'}$, so that the total superpotential is

$$W = W_A + W_C + W_{ACC'} + W_{2/3} \quad .$$

The issue of the doublet-triplet splitting in $SO(10)$ is, in fact, a manifestation of the gauge hierarchy problem which is present in every grand unified theory. In SUSY $SO(10)$, the two Higgs doublets, H_u, H_d , required for the electroweak symmetry breaking, are contained in the vector Higgs multiplets, $H_u \subset \mathbf{5}, H_d \subset \overline{\mathbf{5}}$ of $SU(5)$, which fall into the $\mathbf{10}_H$ representation of $SO(10)$.

This pair of weak doublets must remain massless after the $SO(10)$ breaking at the GUT scale, while their color-triplet partners in the vector Higgs multiplet should obtain superheavy masses. The doublet-triplet splitting is implemented by the Dimopoulos - Wilczek mechanism [8]. This mechanism assumes the existence of a term of the form

$T_1 A T_2$ in the Higgs superpotential and demands the adjoint Higgs multiplet A to have a vev along the $B - L$ direction,

$$\langle A \rangle = \text{diag}(\alpha, \alpha, \alpha, 0, 0) \otimes i\tau_2. \quad (1)$$

The parameter α is of the order of the GUT breaking scale M_{GUT} . If one adds in the superpotential the mass term $M_2 (T_2)^2$, half of the four Higgs doublets contained in T_1, T_2 remain massless and thus the picture of the MSSM Higgs spectrum is revealed at the low energy effective theory. Hence, the doublet-triplet-splitting sector will be assumed to have the following form,

$$W_{2/3} = \lambda T_1 A T_2 + M_2 T_2^2, \quad (2)$$

where λ and M_2 are the massless and GUT scale massive parameters, of this sector, respectively.

The adjoint sector, W_A , is responsible for the Dimopoulos - Wilczek vev $\langle A \rangle$ given in (1), which breaks $SU(5)$ to the Standard Model symmetry preserving $U(1)_{B-L}$ (see Figure 1).

The spinor sector, W_C , of the Higgs superpotential forces the pair of spinor Higgs multiplets $C + \bar{C}$ to get superheavy vevs along the $SU(5)$ singlet direction. In this way, the rank of the group is reduced from 5 to 4, since the $B - L$ symmetry is broken.

Finally, the adjoint-spinor coupling terms, $W_{ACC'}$, are necessary to prevent the manifestation of colored pseudo-Goldstone bosons with small masses, which may destroy the unification of gauge coupling constants and the low energy particle spectrum.

Apart from providing a decent Higgs mechanism, the model just described yields reliable results for the fermion masses [6, 9], including neutrino masses and their oscillations [6, 9], at the electroweak scale by introducing the proper Yukawa terms at the GUT scale.

This paper is organized as follows. In Sec.2, we briefly discuss the proton instability. The expected proton lifetime depends on a superheavy mass M_{eff} which can be expressed in an efficient way as a function of HETs and the gauge coupling constants at M_Z . In Sect.3, we propose a new method to count in the effects of the HETs in the running of the gauge couplings, needed for finding M_{eff} , imposing the experimental constraints from α_{strong} and proton decay. The results of our analysis are presented in Sec.4 and our conclusions are given in Sec.5.

2 Proton Decay

In every GUT model, the baryon number violation is unavoidable and consequently nucleons decay. In $SO(10)$ proton decays through D=5 operators, which are induced via

the exchange of superheavy color triplet Higgsinos in the **10** Higgs multiplet [10–13], with the dominant decay mode being $p \rightarrow \bar{\nu} K^+$. These operators arise from an effective superpotential which is inverse proportional to a mass parameter to be denoted by

$$M_{eff} = \frac{M_3 M'_3}{M_2} = \frac{(\lambda\alpha)^2}{M_2}, \quad (3)$$

where $M_3 M'_3$ are the superheavy color triplet Higgs masses of the vector Higgs multiplets T_1, T_2 . Thus, the expected proton lifetime turns out to be proportional to M_{eff}^2 .

For the dominant decay mode, the decay rate is:

$$\Gamma(p \rightarrow \bar{\nu} K^+) = \sum_{i=e,\mu,\tau} \Gamma(p \rightarrow \bar{\nu}_i K^+). \quad (4)$$

Each of the partial widths in (4) are given by [12–14]:

$$\Gamma(p \rightarrow \bar{\nu}_i K^+) = \left(\frac{\beta_p}{M_{eff}} \right)^2 |A|^2 |B_i|^2 C. \quad (5)$$

The factor β_p denotes the hadronic matrix element between the proton and the vacuum state of the 3 quark operator [15], employed in the appropriate chiral Lagrangian schemes [16]. In our approach, we use [17]

$$\beta_p = (5.6 \pm 0.5) \times 10^{-3} \text{ GeV}^3$$

extracted from lattice gauge calculations. A in (5) depends on quark masses (at 1 GeV) [11] and CKM matrix elements and is given by

$$A = \frac{\alpha_2^2}{2M_W^2} m_s m_c V_{21}^\dagger V_{21} A_S A_L. \quad (6)$$

The first parameter, A_S , represents the short-range renormalization effects between GUT and SUSY breaking scales [11, 13], while the second one, A_L , accounts for the long-range renormalization effects between SUSY scale and 1 GeV [11]. Their values are $A_S \simeq 0.93$, for $m_t = 175$, [18] and $A_L \simeq 0.32$ (2-loop result), [9].

In (5), the B_i s are the functions that describe the dressing of the loop diagrams and are given by the formula

$$B_i = \frac{1}{\sin 2\beta} \frac{m_i^d V_{i1}^\dagger}{m_s V_{21}^\dagger} \left(P_2 B_{2i} + P_3 \frac{m_t V_{31} V_{32}}{m_c V_{21} V_{22}} B_{3i} \right), \quad (7)$$

where B_{ji} is the contribution of the j th generation particles in the loop with

$$B_{ji} = F(\tilde{u}_i, \tilde{d}_j, \tilde{W}) + (\tilde{d}_j \rightarrow \tilde{e}_j). \quad (8)$$

The functions F in (8) contain the corresponding loop integrals [14], with $i = 1, 2, 3$ and $j = 2, 3$, while P_2 and P_3 are inter-generational, CP violating phases given by [14].

$$P_i = e^{i\gamma_i}, \quad \sum_i \gamma_i = 0, \quad i = 1, 2, 3. \quad (9)$$

There exist two distinct limiting cases having to do with the relative contributions of the second and third generation: the destructive interference, occurring for $P_3/P_2 = -1$, and the constructive one when $P_3/P_2 = +1$. We adopt the second case to achieve maximum mixing, and hence smaller, lifetimes that are more tightly constrained by data.

Finally, the factor C in (5) contains chiral Lagrangian factors, which convert a Lagrangian involving quark fields to the effective Lagrangian involving mesons and baryons [19]. Its value has been calculated to be $C = 1.014$, according to the values given in [14].

The current experimental lower bound on proton lifetime from Super-Kamiokande is [20]

$$\tau_{(p \rightarrow \bar{\nu} K^+)} > 1.6 \times 10^{33} \text{ yrs}. \quad (10)$$

For given SUSY inputs, this constrains the value of the parameter M_{eff} , which, as we shall see, depends on the values of the gauge couplings at M_Z and other high energy threshold parameters of the theory. Note that in ref. [13], in the context of the $SU(5)$ model, the color-triplet Higgs boson mass, which is the analogue of M_{eff} in $SU(5)$, is constrained by the precision measurement bounds put on α_{strong} . Following an analogous treatment as in [13], we first solve the 1-loop RGEs for the gauge coupling constants α_i , in the \overline{DR} scheme, from the GUT scale M_{GUT} down to the electroweak scale M_Z and express M_{eff} in terms of $\alpha_i(M_Z)$. In this approach, we count in the high energy thresholds [21, 22] of the superheavy spectrum, as well as the low energy thresholds of all sparticles and heavy SM particles. The resulting expression, for the $SO(10)$ is

$$\frac{M_{eff}}{M_Z} = e^{h(\alpha_i^{-1})} f(x), \quad (11)$$

with

$$h(\alpha_i^{-1}) = \frac{5\pi}{6} [3\alpha_2^{-1}(M_Z) - \alpha_1^{-1}(M_Z) - 2\alpha_3^{-1}(M_Z)].$$

The effect of the low energy thresholds in (11) are encoded within α_i from the low energy boundary conditions that are imposed at M_Z . In fact

$$\begin{aligned} \alpha_1^{-1}(M_Z) &= \frac{3}{5} \alpha_{em}^{-1} \cos^2 \theta_w (1 - \Delta_\gamma + \frac{\alpha_{em}}{2\pi} \ln \frac{M_S}{M_Z}) \\ \alpha_2^{-1}(M_Z) &= \alpha_{em}^{-1} \sin^2 \theta_w (1 - \Delta_\gamma + \frac{\alpha_{em}}{2\pi} \ln \frac{M_S}{M_Z}) \\ \alpha_3^{-1}(M_Z) &= \alpha_{strong}^{-1}(M_Z) |_{\overline{MS}} - \frac{1}{4\pi} + \frac{1}{2\pi} \ln \frac{\tilde{M}_S}{M_Z} \end{aligned} \quad (12)$$

where α_{em} , α_{strong} are the electromagnetic and strong coupling constants respectively, θ_w is the weak mixing angle and \tilde{M}_S , M_S account for the low energy threshold corrections. For further details and for the definition of the remaining quantities in (12) see [23]. At a subsequent stage, one can include a correction factor to (11) to take care of the small two-loop corrections to the gauge coupling running. In our numerical analysis, the two-loop effects are properly counted for since we integrate the 2-loop RGEs of the gauge coupling constants in the \overline{DR} scheme. More details on the method that we employ will be presented in the following section.

The function $f(x)$ in (11) depends only on GUT physics details and, in particular, on the high energy thresholds of the superheavy particles involved. For the case of $SO(10)$, it is found that,

$$f(x) = \frac{9}{16\sqrt{2}} \left[\left(\frac{1+8x^2}{1+x^2} \right)^4 \frac{(1+4x^2)^3}{1+32x^2} \right]^{1/2}. \quad (13)$$

In this expression, the effect of the high energy thresholds of this particular model depend only on the massless, free parameter x , which is defined as

$$x \equiv \frac{\alpha}{2c}, \quad (14)$$

with α , c being connected to the GUT scale vevs of the adjoint and spinor Higgs fields respectively. Obviously, the larger the x , the larger the function $f(x)$ is, facilitating the satisfaction of the proton decay bounds. However, x is naturally expected to be of $\mathcal{O}(1)$ as being the ratio of vevs which are both of order $\sim M_{GUT}$. On these grounds, x cannot be taken arbitrarily large.

For comparison, in the $SU(5)$ model the function $f(x) = 1$ and we recover exactly the result presented in [13].

3 High Energy Thresholds

It is clear from eq.11 that, in order to derive M_{eff} , we need the values of gauge couplings at the electroweak scale. Their values are set by (12) in terms of \tilde{M}_S , M_S . These are not physical masses but rather a convenient device which encodes all information for the low energy supersymmetric thresholds and heavy standard model states. Given the SUSY inputs and α_{em} , α_s , $\sin^2 \theta_w$, we solve the RGEs imposing the gauge coupling unification condition,

$$\alpha_1(M_{GUT}) = \alpha_2(M_{GUT}) = \alpha_3(M_{GUT}) \equiv \alpha_G, \quad (15)$$

but we don't restrict further our analysis by insisting on Yukawa unification. At M_{GUT} , we also impose universal boundary conditions induced by gravity mediated SUSY-breaking

for the soft supersymmetry breaking parameters, although other schemes may be available,

$$m_i = m_0 \quad , \quad M_i = M_{1/2} \quad , \quad A_i = A_0 \quad .$$

Using standard procedure, we calculate the gauge coupling constants at any scale μ below the SUSY thresholds by solving the appropriate RGEs incorporating the effects of the thresholds of all heavy Standard Model particles of mass $m_{SM_i} > \mu$ as well as those of all low energy SUSY particles S_i and superheavy particles H_i with masses $\sim M_{GUT}$ associated with the specific GUT model at hand. The result is

$$\begin{aligned} \alpha_i^{-1}(\mu) &= \alpha_G^{-1}(M_{GUT}) + (2 - \text{loops effects}) \\ &+ \frac{1}{2\pi} (b_i^{SM} + b_i^{SUSY}) \ln \frac{M_{GUT}}{\mu} + \frac{1}{2\pi} \sum_{SM_i} b_i^{SM_i} \ln \frac{\mu}{m_{SM_i}} \\ &+ \frac{1}{2\pi} \sum_{S_i} b_i^{S_i} \ln \frac{\mu}{m_{S_i}} + \frac{1}{2\pi} \sum_{H_i} b_i^{H_i} \ln \frac{M_{GUT}}{m_{H_i}}. \end{aligned} \quad (16)$$

b_i^A are the beta function coefficients of any species A with b_i^{SM} , b_i^{SUSY} being the beta function coefficients of α_i of the SM and low energy supersymmetric modes respectively.

From the evolution of α_i from M_{GUT} to the lowest high energy threshold, M_L , one can easily derive, ignoring momentarily the two loop effects, that

$$\alpha_i^{-1}(M_L) = \alpha_G^{-1}(M_{GUT}) + \frac{1}{2\pi} b^{GUT} \ln \frac{M_{GUT}}{M_L} + \frac{1}{2\pi} \sum_{H_i} b_i^{H_i} \ln \frac{M_L}{m_{H_i}}, \quad (17)$$

where $b^{GUT} \equiv b^{SM} + b^{SUSY} + b^H$. By defining

$$\alpha_G^{-1}(M_L) \equiv \alpha_G^{-1}(M_{GUT}) + \frac{1}{2\pi} b^{GUT} \ln \frac{M_{GUT}}{M_L}, \quad (18)$$

which represents the running from M_{GUT} to M_L , if HETs are ignored, and by using

$$c_i \equiv \frac{1}{2\pi} \sum_{H_i} b_i^{H_i} \ln \frac{M_L}{m_{H_i}} \quad (19)$$

equation (17) can be cast in the form,

$$\alpha_i^{-1}(M_L) = \alpha_G^{-1}(M_L) + c_i. \quad (20)$$

where the effect of HET is included within c_i .

Eqs. (20) can serve as boundary condition at the lowest HET, M_L that takes into account the effects of all HETs, which are included within the constant c_i . Between M_L and the electroweak scale $\mu = M_Z$ no high energy thresholds are present and RGEs run as usual.

The importance of the adoption of the parametrization (19) lies on the fact that the three c_i 's carry all information on the masses of the non-singlet superheavy fields of the model which contribute to the HETs in the running from M_Z to M_L and vice versa. For any set of the model parameters, say p_j , we assign a “vector” in a five dimensional space $\vec{c} = (c_1, c_2, c_3, M_L, M_{GUT})$, which includes, except c_i , the values of the maximum, M_{GUT} , and lowest high energy mass, M_L . For instance, in the version of the $SO(10)$ model we are considering, the number of the parameters p_j is ten and for any point in this ten-dimensional parameter space there correspond twenty-five correlated superheavy masses from which we determine M_{GUT} , M_L and c_i s through their definitions in (19). Further, in order to utilize c_i as inputs, we use a random sample generator, which assigns random numbers to the GUT parameters p_j . In this way, random points $\vec{p} \equiv (p_1, p_2, \dots, p_N)$ are drawn in the model parameter space and each of this is mapped to a \vec{c} defined before. Consequently, our analysis is fully constrained from the random sample results and instead of dealing with a large number of GUT parameters and masses, we only have a few to consider in our analysis, namely $c_1, c_2, c_3, M_L, M_{GUT}$, which define \vec{c} . The random procedure actually makes a selection by mapping the parameter space to a rather confined region, at least in the $SO(10)$ model, which is spanned by the vectors \vec{c} . Then, within this region, points satisfying the experimental criteria can be sought and the region shrinks even more. Consequently, one avoids time-consuming scans over a multidimensional (10-dimensional in $SO(10)$) parameter space, since the random procedure has already selected the points \vec{c} which meet the criteria. In this way we have found a very convenient way to parametrize the effect of HET, which is applicable to almost any GUT model, using the variables \vec{c} .

We will now discuss in more detail the numerical procedure we follow. For any input point in the space of the randomly generated vectors, \vec{c}_{in} , we pick up the points c_1^{in}, c_2^{in} and by running the 2-loop RGEs upwards, starting from M_Z , we determine the values of M_L and $\alpha_G(M_L)$ where the boundary condition (20) are satisfied. By (18) the value of $\alpha_G(M_{GUT})$ is also determined. Note that in this way the input value, M_L^{in} , is not the same with the extracted value, M_L . Subsequently, we define c_3 so that

$$c_3 = \alpha_3^{-1}(M_L) - \alpha_G^{-1}(M_L). \quad (21)$$

and relation (20) is satisfied for the coupling α_3 . That done, the initial point \vec{c}_{in} , with c_i^{in}, M_L^{in} , has moved to another with coordinates $c_1^{in}, c_2^{in}, c_3, M_L, M_{GUT}^{in}$, i.e. the values of c_3 and M_L have been only changed. This procedure is repeated in each iterative step from the electroweak to the GUT scale, in the usual manner, until convergence has been obtained. In each iteration step, c_1, c_2 are also corrected to meet the unification criteria but these corrections are small. Thus, at the end, we get a final point, \vec{c}_{fin} , which is a

successful point if it belongs to the set of the randomly generated vectors \vec{c} or unsuccessful and hence discarded if it lies outside the region spanned by \vec{c} points. In order to test the correctness of our method, we check, at the end, if a successful point maps to itself, modulo small differences due to numerical accuracies. This procedure will be explained and quantified in more detail later.

Obviously, the set of successful points that pass the unification test will be reduced if additional physics constraints are imposed, like, for instance, bounds put by proton decay.

The advantage of the method is that the running, from M_Z to M_L , of the couplings involved is done without the effect of the HET in the RGEs. Their effect is taken into account by the boundary condition (20), which incorporates all the HET information within c_i 's.

The boundary conditions for the couplings and soft mass parameters are imposed at the unification scale, and, in the running from M_{GUT} to M_L , the HET play an essential role. Since, in our approach, we want to treat HET collectively, through quantities similar to c_i , without knowledge of their precise values, we use the two-loop RGEs without the contribution of the superheavy particles, which are known. However, in order to include the effect of the HETs, at the end we correct each derived quantity at the scale M_L as

$$F^{cor}(M_L) = F(M_L) + \Delta_F.$$

The added quantity, Δ_F , depends on c_i , on the beta function coefficients $b_i^H \equiv \sum_{H_i} b_i^{H_i}$ of the superheavy modes that are known and on $\ln(M_{GUT}/M_L)$. The correction Δ_F is different for each quantity F and, for its knowledge, the one-loop explicit dependence of the RGE of the F need to be known. In particular, if

$$\frac{dF}{d\ln Q} = \sum_i G_i \alpha_i + \dots,$$

where the ellipses denote contributions not explicitly dependent on the gauge couplings, the correction is

$$\Delta_F = \frac{\alpha_G^2}{4\pi} \ln\left(\frac{M_{GUT}}{M_L}\right) \sum_i G_i(M_{GUT}) \left[\ln\left(\frac{M_{GUT}}{M_L}\right) b_i^H + 2\pi c_i \right].$$

This is a valid approximation provided that the lowest, M_L , and the highest, M_{GUT} , threshold are not far apart. In particular, $\frac{M_L}{M_{GUT}} < 10^{-3}$ is demanded. From the random samples, we find that on an average $\log \frac{M_L}{M_{GUT}} \simeq 2.7$ and thus the approximation is more than satisfactory.

With these in mind, we calculate couplings and masses at the electroweak scale in the ordinary manner with the values of the gauge couplings determined by the electroweak precision measurements, [20], namely the effective mixing angle, $\overline{\sin_f^2 \hat{\theta}}(M_Z)(\overline{MS}) = 0.23152(14)$,

the value of the strong coupling constant: $\alpha_s(M_Z) = 0.1176(20)$ and the electromagnetic coupling α_{em} . Note that the experimentally measured effective mixing angle $\overline{\sin_f^2 \hat{\theta}}$ is not the same with $\sin^2 \theta_w$ appearing in (12), which is defined as ratio of couplings in the \overline{DR} scheme. Actually, the two are related by

$$\overline{\sin_f^2 \hat{\theta}} = \sin^2 \theta_w (1 + \Delta k_f),$$

where Δk_f is calculated by the effective $Zf\overline{f}$ coupling.

The minimization conditions are solved with all one-loop effective potential corrections and the dominant two-loop QCD and top Yukawa corrections taken into account. The value of the $|\mu|$ parameter is then determined by the minimization conditions and $\tan \beta$ is input. Therefore, apart from the particular treatment of HETs, the procedure is the standard one encountered in the constrained MSSM models. As far as proton decay is concerned, for given SUSY inputs, m_0 , $M_{1/2}$, A_0 , $\tan \beta$, we derive M_{eff} , from (11), and B_i 's, in eq.(7), which both affect the proton decay. Then proton lifetime is calculated and it provides an additional constraint. Since the dependence of M_{eff} on HETs is explicit only on the quantity x , defined by eq. (14), to facilitate the analyses we shall pick slices of fixed values of x , in the space of random points, within which M_{eff} is almost constant.

4 Numerical Analysis - Results

We follow the procedure described in Sec.2 and 3, in order to delineate the acceptable parameter region of the model at hand, which complies with electroweak precision data and proton decay constraint. Satisfaction of the experimental bounds on the strong coupling constant α_{strong} , by itself, imposes severe constraints, as we shall see, in conjunction with precision measurements and unification conditions.

In order to facilitate the analysis, we generate random samples of randomly generated points \vec{c} for which M_{GUT} is fixed. In our analysis, we present results for $M_{GUT} = 2 \cdot 10^{16} GeV$ but higher values are not excluded, yielding qualitatively similar results. However, perturbativity limits on Yukawa and gauge couplings poses upper bounds on higher M_{GUT} values and hence such large values are not considered. Besides, we select points defining "slices" in the space of \vec{c} vectors for which the ratio x defined in eq. (14) is $x = 5$. In fact, we have found that a larger x satisfies the proton decay constraint easier, while a smaller one fails on both proton decay and α_{strong} constraints. In the following, for a more clearer presentations, only 1000 points are displayed in each Figure.

In general, the effective weak - mixing angle, denoted in the Figures by s_f , takes values with error less than 3σ over all the parameter space, but the strong coupling constant prefers rather low values of SUSY breaking parameters. This is expected since for high

values SUSY is absent, due to decoupling, and, in this case, we deal with a conventional GUT model for which gauge coupling constant unification is hard to achieve. On the other hand, high SUSY breaking parameters and, in particular $M_{1/2}$, which affects wino masses and in turn Eq. (8), shrink the range of the allowed values of M_{eff} , by proton decay bounds, leaving out a small number of the initial randomly generated points that pass successfully the proton decay and precision data tests. This is the reason only relatively small values for the SUSY breaking parameters are considered, $m_0, M_{1/2} \leq 1.5 TeV$.

4.1 The α_{strong} and proton decay constraints

We come to the point of examining the dependence of the strong coupling constant α_{strong} on the supersymmetric and HET parameters. We first observe its variation with changing m_0 and $M_{1/2}$. In Figure 2-5, we display the pairs of c_1, c_2 as they are randomly generated. The value of the unification scale has been taken $M_{GUT} = 2 \cdot 10^{16} GeV$ and on naturalness reasons all high energy parameters having dimension of mass are randomly generated with values differing from M_{GUT} by at most three orders of magnitude. Although these parameters have been randomly generated from the independent parameters of the model, in the way prescribed earlier, they are correlated as shown clearly in the Figures. Therefore, successful points ought to be within the diagonal stripe displayed in these Figures.

The black points represent those pairs of c_1, c_2 that fail even to give unification at the quoted M_{GUT} , after the 2 - loop running of the RGEs. For the green points, unification has been achieved but the value of α_{strong} is more than 4σ away. The magenta points yield α_{strong} with error smaller than 4σ , and the yellow region is the subset of magenta points corresponding to values of α_{strong} with the smallest possible error $< 2\sigma$.

In Figures 2 to 5, we vary the input values of m_0 and $M_{1/2}$, as shown on each Figure, by increasing either one, or both, of $m_0, M_{1/2}$, but keeping $M_{GUT}, \tan\beta$ and A_0 fixed. In Figure 6, we display the analog of Figure 2 but with c_2 replaced by c_3 . A correlation of c_1 and c_3 is also observed with points that are more widely scattered.

By raising the values of m_0 and $M_{1/2}$, we have observed a considerable decrease of the number of random sample points that result in an acceptable α_{strong} value. The yellow region shrinks and shifts slightly towards smaller values of c_2 and eventually disappears, as is the case in the displayed Figures 3 to 5. In those cases, the deviation of the theoretical from the experimental value of α_{strong} never becomes less than 2σ . In Figure 4, by increasing the value of m_0 , keeping $M_{1/2} = 800 GeV$ as in Figure 2, the yellow and the magenta regions disappear, which means that the predicted theoretical values for α_{strong} are outside the experimental limits. Therefore, to be within experimental limits, the values

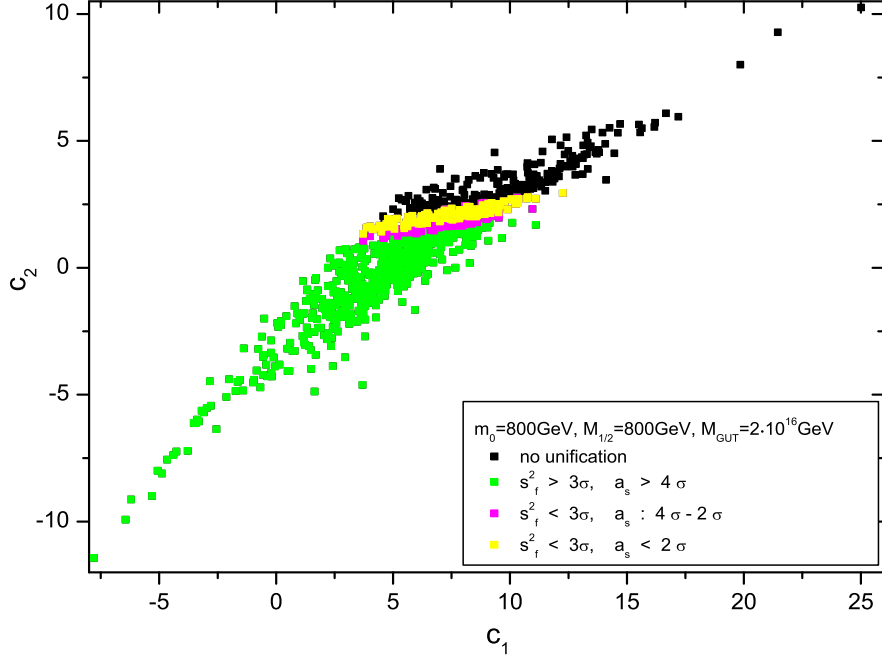


Figure 2: In this Figure $\tan \beta = 10$ and $A_0 = 100$ GeV, with m_0 , $M_{1/2}$ and M_{GUT} as displayed. For a detailed description of the Figure see main text.

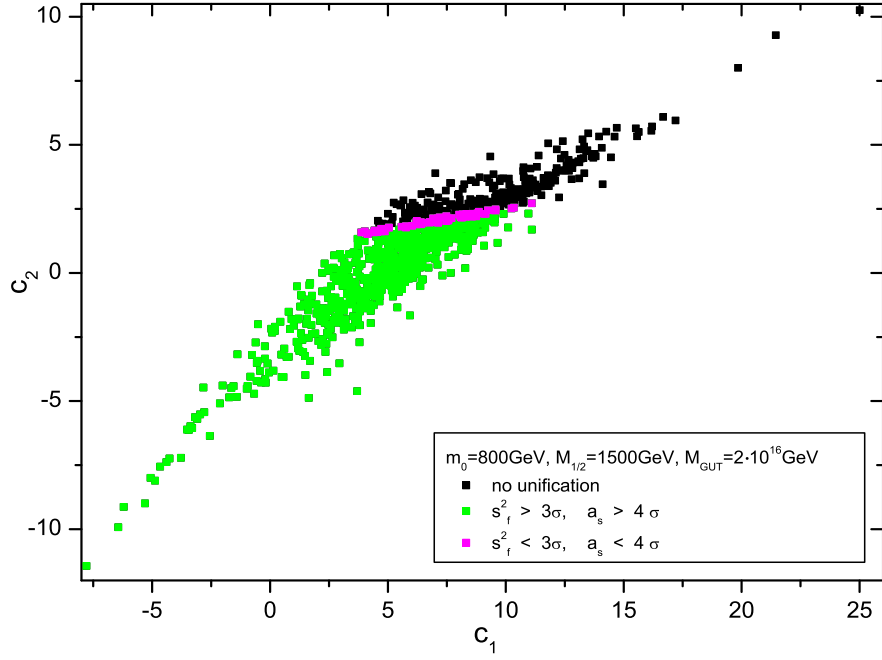


Figure 3: As in Figure 2.

of $M_{1/2}$ and primarily m_0 should be kept central to small. The α_{strong} constraint is best met in a region of the $m_0 - M_{1/2}$ plane bounded by values of m_0 up to 1000 GeV and $M_{1/2}$

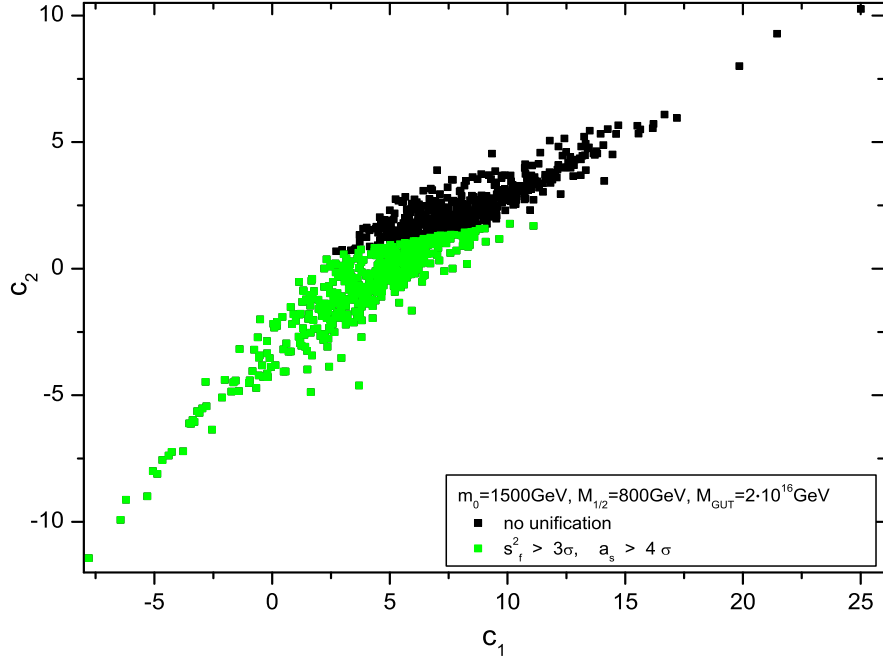


Figure 4: As in Figure 2.

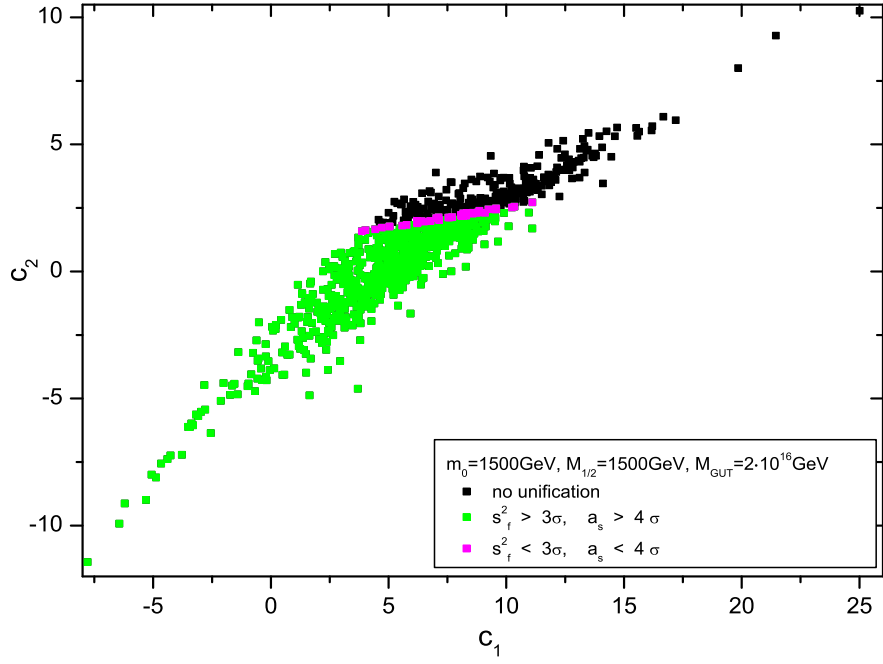


Figure 5: As in Figure 2.

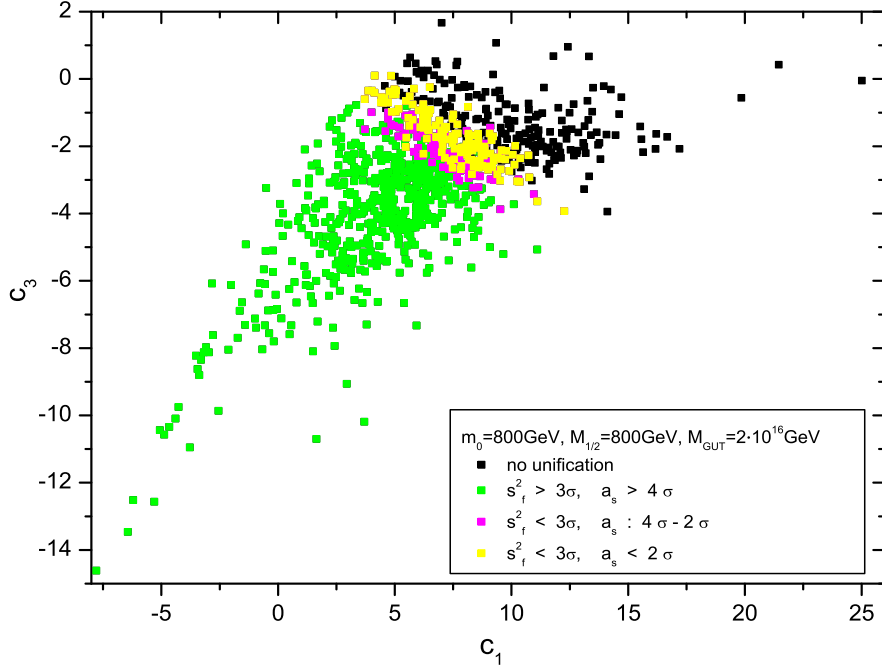


Figure 6: As in Figure 2.

up to 1300 GeV. For larger values of m_0 up to 1400 GeV, we should choose $M_{1/2}$ between 900 and 1300 GeV at most and for larger values of m_0 up to 1500 GeV, we should go for small m_0 around 500 GeV. This conclusion was rather expected since for large values of m_0 and $M_{1/2}$, exceeding 1 TeV, the MSSM and the Standard Model, due to decoupling, give almost the same predictions for the unification of coupling constants, where SM fails to yield a satisfactory unified picture.

Based on the most recent experimental bound on proton lifetime (10), the lower bound on its lifetime translates into a lower bound on the mass parameter M_{eff} that controls the proton decay width. This, denoted by $M_{eff}(exp)$, can be extracted from eq. (5) and it is defined below. We perform these calculation for every randomly generated pair of c_1, c_2 and the constraint of proton decay is satisfied provided that

$$M_{eff}(th) > M_{eff}(exp) \equiv \beta_p |A| \sqrt{\tau_b C \sum_i |B_i|^2}, \quad (22)$$

where τ_b is the bound in (10) and $M_{eff}(th)$ is read from (11).

Running the RGEs we find points for which (22) is satisfied and the resulting $M_{eff}(th)$ yields a proton lifetime in the range $10^{34} - 10^{37}$ years. In Figure 7, we illustrate this constraint for the case of $m_0 = M_{1/2} = 800$ GeV, by coloring in gray the pairs of c_1, c_2 which fulfill (22) and in black the rest of those. These points overlap with the majority of the points that yield gauge coupling unification with values of α_{strong} within the 2σ experimental

range. Raising of m_0 and/or $M_{1/2}$ results to an homogeneous reduction of the gray region around a central point. Besides, the unilateral increase of m_0 keeping $M_{1/2}$ rather small leads to experimentally unacceptable proton decay rates.

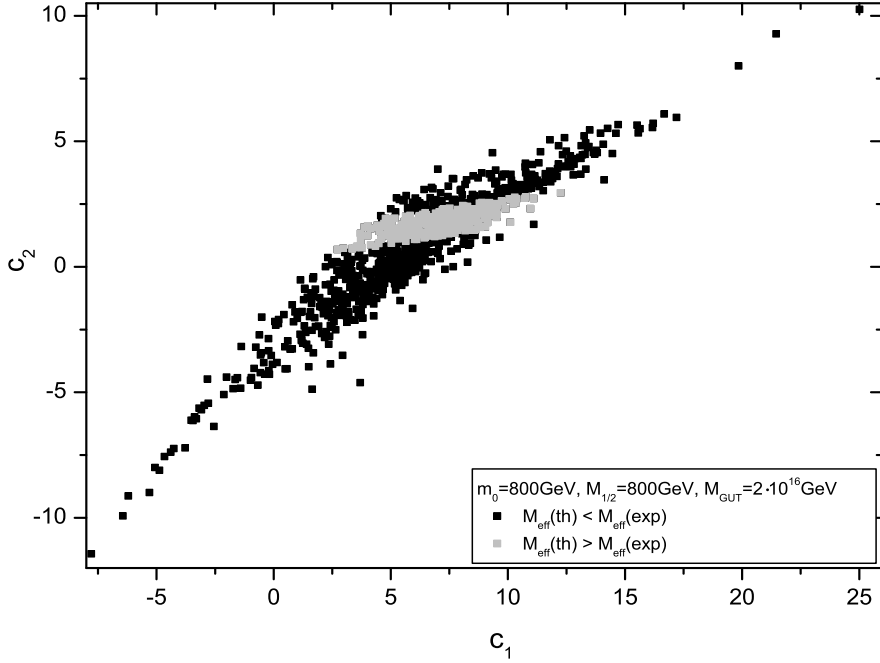


Figure 7: In this Figure $\tan\beta = 10$ and $A_0 = 100$ GeV, with $m_0, M_{1/2}, M_{GUT}$ as quoted. For a detailed description of the Figure see main text.

The results depend on the unification scale M_{GUT} , which is an input in our analysis. For α_{strong} , raising M_{GUT} by almost one order of magnitude ($M_{GUT} = 9 \cdot 10^{16}\text{GeV}$) broadens the yellow region of Figure 2 which now includes smaller values for c_1, c_2 . We note that almost half of the yellow points yield α_{strong} within 1σ error. Taking the same high value for M_{GUT} , in the case of the proton decay constraint, results to the same behavior. In fact, the gray region of Figure 7 moves towards smaller values of c_2 , while it reaches a wider range of values for c_1 . It is interesting to note that half of the points which bring unification of the coupling constants fulfill the proton decay constraint for $M_{GUT} = 9 \cdot 10^{16}\text{GeV}$, while for $M_{GUT} = 2 \cdot 10^{16}\text{GeV}$ the corresponding rate is 40%. Thus, by pushing M_{GUT} to higher value provides easier satisfaction of the constraints. As far as A_0 is concerned, this parameter does not seem to play a significant role in our analysis.

Our findings depend also on the value of $\tan\beta$. A change of $\tan\beta$ from 10 to 45 causes a small decrease, ranging from 5 to 15%, in the number of points which succeed to give unification and, at the same time, shrinks their range of output values. A likely

explanation for this is that a high value of $\tan \beta$ increases the chance of a Landau pole to appear during the running of the RGEs. Also, the raise of $\tan \beta$ bounds the points which give α_{strong} with error more than 4σ to have only positive c_1 and only negative c_3 . On the other hand, with a large $\tan \beta$ the number of points which give α_{strong} with error less than 4σ (or 2σ for $m_0 = M_{1/2} = 800$ GeV) slightly increases. As far as the proton decay constraint is concerned, the points which satisfy (22) show a considerable decrease, which starts from 22% for $m_0 = M_{1/2} = 800$ GeV and reaches a 100% for $m_0 = 1500$ GeV and $M_{1/2} = 800$ GeV. This was rather expected since B_i in (22) depends on $\frac{1}{\sin 2\beta}$. Hence, a change of $\tan \beta$ from 10 to 45 quintuples or so the values of $M_{eff}(exp)$ leaving, at the same time, the values of $M_{eff}(th)$ almost unchanged. Therefore, the chance of satisfying (22) decreases. Overall, a change of $\tan \beta$ from 10 to 45 makes the satisfaction a harder task.

4.2 Convergence of results

In section 3, we pointed out that, in general, there are differences between the final points $\vec{c}_{fin} = \{c_1^{fin}, c_2^{fin}, c_3^{fin}, M_L^{fin}\}$, stemming from the running of the RGEs (output values), and the initial (input values) $\vec{c}_{in} = \{c_1^{in}, c_2^{in}, c_3^{in}, M_L^{in}\}$, generated from the random sample, owing to the corrections imposed to achieve unification at the given M_{GUT} . For the case of c_1 and c_2 , there is a close agreement between the input and output values but the same cannot be asserted for c_3 as discussed in section 3. Actually, this deviation is expected since the c_3 parameter is strongly correlated to α_{strong} and is forced to make the strong coupling be compatible with the unification scale that is determined by the couplings $\alpha_{1,2}$. This is implemented by the shift of eq. (21), resulting to c_3^{fin} , which is always towards higher values comparing to input c_3^{in} . This is also the case for $c_{1,2}^{in}$ and M_L^{in} , which are also shifted towards higher values but to a much lesser extend.

Focusing only on the ability of the random sample points to accomplish unification of the gauge couplings, without any other experimental constraint, an overlapping region of both input and output points must exist for the model to be successful. We have found that the gap between the initial and final points augments by increasing m_0 and by reducing M_{GUT} .

The situation becomes more constrained if we simultaneously demand satisfaction of both α_{strong} and proton decay constraints. For instance in Figure 8 we display in gray the points of c_1, c_3 as they are randomly generated. Actually, this represents a magnification of the central and upper area of Figure 6. The green points represent the output values c_1^{fin}, c_3^{fin} of the gray input points c_1^{in}, c_3^{in} which yield values of α_{strong} with error higher than 4σ . The magenta points are the corresponding points which yield α_{strong} with smaller

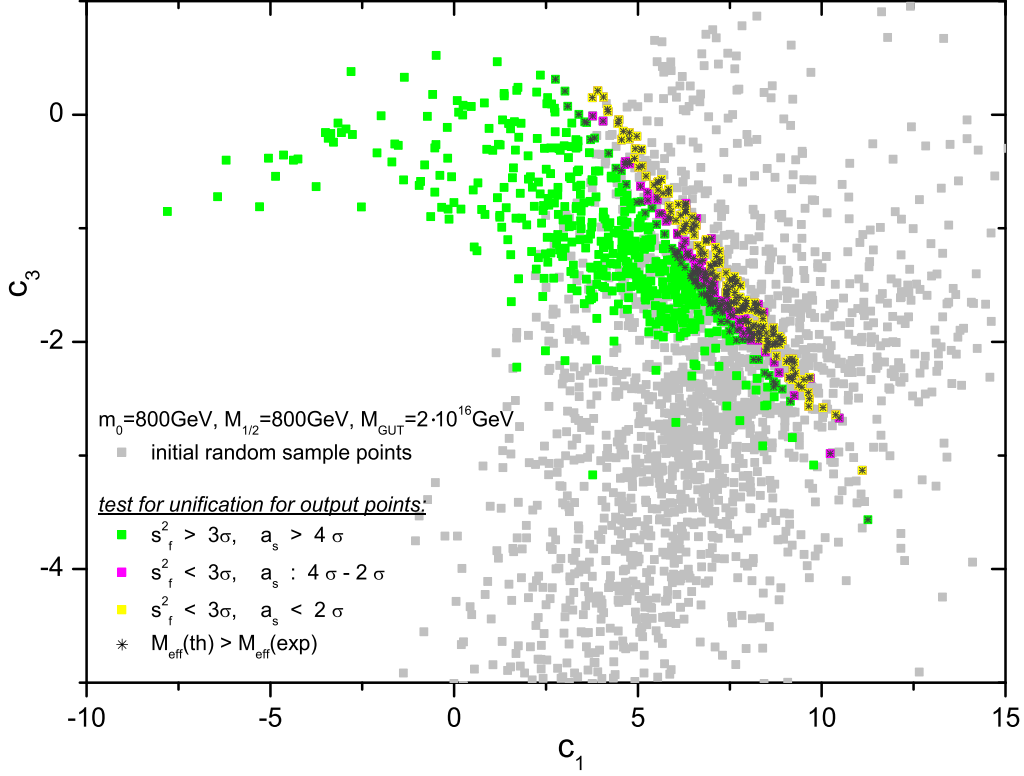


Figure 8: $\tan\beta = 10$ and $A_0 = 100$ GeV, with $m_0, M_{1/2}, M_{GUT}$ as quoted. For a detailed description of the Figure see main text.

error, between 4σ and 2σ , while the yellow points give α_{strong} with error less than 2σ . The gray crosses designate those output points that satisfy the proton decay constraint.

We perform a "second" run using as inputs the elements of the previously produced output groups. In this run, we first check whether these points are mapped to themselves as they should. These are likely to be successful points provided they are subset of the initial randomly generated points. Obviously, only a subset of those survives, if it does at all, and this comprises the set of successful points. In order to check numerically whether a final point belongs to the set of the initial points, we define the "distance" χ_i of the point \vec{c}_{fin} from any \vec{c}_{in}^i of the randomly generated points

$$\chi_i \equiv \left| \frac{c_1^{fin} - c_1^{in,i}}{c_1^{in,i}} \right| + \left| \frac{c_2^{fin} - c_2^{in,i}}{c_2^{in,i}} \right| + \dots + \left| \frac{c_5^{fin} - c_5^{in,i}}{c_5^{in,i}} \right|.$$

The minimum of these $\chi = \min\{\chi_i\}$ defines the distance of \vec{c}_{fin} from the set of the randomly generated points and if zero it means that the final point coincides with one of the random points that were initially created. In practice, the smallness of χ indicates that the particular point is successful in the sense that it belongs to the $SO(10)$ model

and in addition it agrees with the experimental results.

In our analysis and with one million random points, we have found that points with $\chi \leq 0.1$ are acceptable by the model.

This analysis certainly depends on the SUSY inputs. In the $m_0 - M_{1/2}$ plane, successful points are found for values of m_0 and $M_{1/2}$ reaching roughly 1000 GeV. If one keeps the higher end of $M_{1/2}$ values constant, the restrictions are satisfied altogether for values of m_0 up to approximately 1200 GeV. If we loosen the restriction for χ to $\chi \leq 0.2$, keeping the other two constraints untouched, our successful region matches the one described in subsection 4.1. This findings supports not only our method but also the $SO(10)$ model we have followed on the ground of satisfying α_{strong} and proton decay constraints.

5 Conclusions

We have presented a new approach towards treating in a collective way the large number of HET encountered in GUTs quantities by using a random sample technique. According to this technique the large number of the GUTs parameters, defining the high energy sector and hence the threshold masses, are mapped to a few properly defined parameters encoding all the information associated with the renormalization group running of the various quantities involved from the unification scale down to electroweak energies. This method is simple and efficient since :

1. It avoids unnecessary runnings, occurring in the conventional scheme, where for each point in the multidimensional parameter space one has to solve numerically the RGEs.
2. The parameter space is mapped to properly defined quantities, associated with the running of the gauge couplings, which collectively include enough information through which regions favoured by precision data on gauge couplings are easily located.
3. The RG equations are solved without the inclusion of High Energy Thresholds and their effect is duly taken into account by changing appropriately the boundary conditions at the lowest of the high energy thresholds and at the Unification scale.
4. This scheme is fast and accurate if the lowest, M_L , and the highest, M_{GUT} , of the high energy threshold are separated by at most three orders of magnitude, $M_L/M_{GUT} < 10^{-3}$.

We applied this technique to an $SO(10)$ -based model where only five parameters ($c_{1,2,3} \tan \theta$ and M_L) embody all information associated with the HETs. Our analysis shows that this method is both convenient and efficient. We test it and demonstrate that there exists a confined region of c_i s values which yields results in agreement with the limitations imposed by precision data and coupling constant unification, as well as proton decay constraints. These regions are favored by central to small values of m_0 and $M_{1/2}$ in the the region of 500 GeV –1.5 TeV and are suppressed for large $\tan \beta$ due mainly to proton decay constraints. The effect of the common trilinear coupling A_0 is small provided it lies in the TeV range.

Acknowledgements

The author is grateful to A.B. Lahanas for extensive discussions, critically reading the manuscript and continuous support during this effort. The author wishes to acknowledge support by the European Union through the fp6 Marie-Curie Research and Training Network Heptools (MRTN-CT-2006-035505). She acknowledges also partial support from the University of Athens Special Research Account.

References

- [1] H. Georgi, Particles and Fields, *Proceedings of the APS Div. of Particles and Fields*, ed. C. Carlson, p.575(1975);
H. Fritzsch and P. Minkowski, Ann. Phys. 93(1975) 193.
- [2] M. Gell-Mann, P. Ramond and R. Slansky, in Supergravity, edited by P. van Nieuwenhuizen and D.Z Freedman, (North-Holland, Amsterdam, 1979);
T. Yanagida, in Proceedings of the Workshop on the Unified Theory and the Baryon Number of the Universe, edited by O. Sawada and A. Sugamoto (KEK report No. 79-18, Tsukuba, Japan, 1979);
R.N. Mohapatra and G. Senjanovic, Phys. Rev. Lett. 44 (1980) 912 .
- [3] T. Blazek, R. Dermisek and S. Raby, Phys. Rev. Lett. 88 (2002) 111804 ; *ibid*, Phys. Rev. D 65 (2002) 115004.
- [4] S.M. Barr, Stuart Raby, Phys. Rev. Lett. 79 (1997) 4748.
- [5] K.S. Babu, S.M. Barr, Phys. Rev. D50 (1994) 3529; D51 (1995) 2463;
K.S. Babu, Q. Shafi, Phys. Lett. B357 (1995) 365.

- [6] Carl H. Albright, K.S. Babu, S.M. Barr, Phys. Rev. Lett. 81 (1998) 1167;
Carl H. Albright, S.M. Barr, [hep-ph/0007145].
- [7] K.S. Babu, R.N. Mohapatra, Phys. Rev. Lett. 70 (1993) 2843;
H.S. Goh, R.N. Mohapatra, Siew-Phang Ng, Phys. Lett. B570 (2003) 215.
- [8] S. Dimopoulos, F. Wilczek, *The Unity of the Fundamental Interactions*, Proceeding of the 19th Course of the International School of Subnuclear Physics, Erice, Italy, 1981, edited by A. Zichichi (Plenum Press, New York, 1983).
- [9] K.S Babu, Jogesh C. Pati and Frank Wilczek, Nucl. Phys. B566 (2000) 33;
J. C. Pati, Int. J. Mod. Phys. A **18** (2003) 4135.
- [10] S. Dimopoulos, S. Raby, F. Wilczek, Phys. Lett. B112 (1982) 133.
- [11] J. Ellis, D.V. Nanopoulos, S. Rudaz, Nucl. Phys. B202 (1982) 43.
- [12] P. Nath, R. Arnowitt, Phys. Rev. D49 (1994) 1449; *ibid* Phys. Rev. D 38 (1988) 1479;
P. Nath, A.H Chamseddine, R. Arnowitt, Phys. Rev. D32 (1985) 2348.
- [13] J. Hisano, H. Murayama, T. Yanagida, Nucl. Phys. B402 (1993) 46; *ibid*
Phys.Rev.Lett. 69 (1992)1014.
- [14] P. Nath, R. Arnowitt, Phys. Atom. Nucl. 61 (1998) 975; *ibid* [hep-ph/9309277].
- [15] J. Brodsky, J. Ellis, S. Hagelin, C.T. Sacharajda, Nucl. Phys. B238 (1984) 561.
- [16] M. Claudson, M.B. Wise, L.J. Hall, Nucl. Phys. B195 (1982) 297.
- [17] M.B. Gavela et al, Nucl. Phys. B312 (1989) 269.
- [18] K. Turzynski, JHEP 0210 (2002) 044.
- [19] S. Chadha, M. Daniels, Nucl. Phys. B229 (1983) 105.
- [20] C. Amsler *et al.* [Particle Data Group], Phys. Lett. B **667** (2008) 1.
- [21] S. Weinberg Phys. Lett. B91 (1980) 51.
- [22] L. Hall, Nucl. Phys. B178 (1981) 75.
- [23] A. Dedes, A.B. Lahanas, J. Rizos, K. Tamvakis, Phys. Rev. D55 (1997) 2955.